

Universitatea Națională de Știință și Tehnologie
POLITEHNICA din București
Facultatea de Inginerie Chimică și Biotehnologii
Școala Doctorală de Inginerie Chimică și Biotehnologii



ABSTRACT OF DOCTORAL THESIS

*Hybrid lipid nanocarriers containing different
plant active principles with antitumor
potential*

PhD student: Ing. Robert-Andrei ȚINCU

PhD supervisor: Prof. Dr. Ioana LĂCĂTUȘU

Bucharest

-2025-

Tabel of contents of the doctoral thesis

LIST OF ABBREVIATIONS	1
LIST OF FIGURES	3
LIST OF TABLES	7
INTRODUCTION	8
CHAPTER I: NANOSTRUCTURED LIPID CARRIERS – DELIVERY SYSTEMS FOR BIOLOGICALLY ACTIVE COMPOUNDS	13
1.1. DELIVERY SYSTEMS FOR ACTIVE INGREDIENTS	13
1.2. NANOSTRUCTURED LIPID CARRIERS (NLC) – GENERAL OVERVIEW	18
1.3. METHODS FOR OBTAINING NLC	22
1.4. APPLICATIONS OF NANOSTRUCTURED LIPID CARRIERS IN ONCOLOGY	28
CHAPTER II: STRATEGIES FOR NLC SURFACE MODIFICATION TO IMPROVE TARGETING OF AFFECTED CELLS... 33	33
2.1. CHARACTERISTICS OF CANCER CELLS	33
2.2. MECHANISMS AND TYPES OF ANTITUMOR TARGETING	35
2.3. EXAMPLES OF NLCs COATED OR FUNCTIONALIZED WITH VARIOUS LIGANDS FOR TARGETED TUMOR CELL ACTION	37
CHAPTER III: ALBUMIN-BASED SYSTEMS WITH APPLICATIONS IN THE TREATMENT OF ONCOLOGICAL DISEASES	43
3.1. ALBUMIN: GENERAL CHARACTERISTICS	43
3.2. SPECIFIC PROPERTIES OF ALBUMIN FOR MEDICAL APPLICATIONS	45
3.4. ALBUMIN-SPECIFIC CELL RECEPTORS	49
3.5. ALBUMIN-BASED DRUG DELIVERY SYSTEMS	50
CHAPTER IV: PHYTOCHEMICAL PRINCIPLES. STRUCTURAL AND PHARMACOLOGICAL ASPECTS, AND STRATEGIES TO IMPROVE THEIR BIOAVAILABILITY	64
JUSTIFICATION OF THE RESEARCH TOPIC. GENERAL OBJECTIVES	69
CHAPTER V: MATERIALS AND METHODS	72
5.1. MATERIALS AND REAGENTS	72
5.2. SYNTHESIS OF HYBRID NLC	77
5.3. STRUCTURAL, MORPHOLOGICAL, AND FUNCTIONAL CHARACTERIZATION OF NLC SYSTEMS	80
5.4. ISOLATION AND CHARACTERIZATION OF PIPERINE FROM BLACK PEPPER BERRIES	99
5.5. SYNTHESIS AND CHARACTERISATION OF MENTHYL LAURATE	100
CHAPTER VI: EXTRACTION OF PIPERINE AND SYNTHESIS OF MENTHYL LAURATE	101
6.1. EXTRACTION OF PIPERINE FROM BLACK PEPPER BERRIES	102
6.2. SPECTROSCOPIC ANALYSIS OF PIPERINE	106
6.3. SYNTHESIS AND CHARACTERIZATION OF MENTHYL LAURATE	113
CHAPTER VII: PRELIMINARY NLC COMPOSITION OPTIMIZATION STUDIES	124
7.1. OPTIMIZATION OF NLC FORMULATIONS FOR PIPERINE ENCAPSULATION	125
7.2. OPTIMIZATION OF NLC FORMULATIONS FOR <i>SAMBUCUS NIGRA</i> ENCAPSULATION	129
CHAPTER VIII: NOVEL BOVINE SERUM ALBUMIN-DECORATED–NANOSTRUCTURED LIPID CARRIERS ABLE TO MODULATE APOPTOSIS AND CELL-CYCLE RESPONSE IN OVARIAN, BREAST, AND COLON TUMORAL CELLS ..	136
8.1. OPTIMIZATION OF SURFACTANT AND ALBUMIN COMPOSITION FOR NEW BSA -NLC FORMULATIONS	137

8.2. LIPID NANOCARRIERS COATED WITH BOVINE SERUM ALBUMIN AND LOADED WITH PIPERINE.....	143
8.3. <i>IN VITRO</i> TESTING OF CONVENTIONAL AND BSA-COATED NLCs	148
8.4. ANTITUMOR PROPERTIES OF NLC-PIP COMPARED TO BSA-DECORATED NLC-PIP	150
8.5. CONCLUSIONS.....	162
CHAPTER IX: HYBRID ALBUMIN-DECORATED LIPID-NANOCARRIER-MEDIATED DELIVERY OF POLYPHENOL-RICH <i>SAMBUCUS NIGRA</i> L.....	164
9.1. PHYSICO-CHEMICAL CHARACTERIZATION OF NLCs LOADED WITH <i>SAMBUCUS NIGRA</i> EXTRACT.....	165
9.2. FTIR AND FLUORESCENCE SPECTROSCOPY ANALYSIS OF NLC- <i>SAMBUCUSN</i> -BSA	172
9.3. <i>IN VITRO</i> EVALUATION OF ANTIOXIDANT ACTIVITY	175
9.4. <i>IN VITRO</i> TESTING OF THE ANTI-TUMOR EFFICACY OF OBTAINED NLC SYSTEMS	178
9.5. CONCLUSIONS.....	199
CHAPTER X: FINAL CONCLUSIONS AND PERSONAL CONTRIBUTIONS.....	201
10.1. FINAL CONCLUSIONS	201
10.2. ORIGINAL CONTRIBUTIONS	206
PUBLICATIONS.....	209
REFERENCES	210

ABBREVIATIONS LIST

ABBREVIATION	DEFINITION
ABTS	2,2'-Azino-Bis(3-Ethylbenzothiazoline-6-Sulfonic Acid)
AOT	Dioctyl Sodium Sulfosuccinate
CB	Coconut Butter
CI	Cells Index
Cis-Pt	Cisplatin
DCC	N,N'-Dicyclohexylcarbodiimide
DDS	Drug Delivery Systems
DLS	Dynamic Light Scattering
DMAP	N,N-Dimethylaminopiridine
DMEM	Dulbecco's Modified Eagle's Medium
DMSO	Dimethylsulfoxide
DOX	Doxycyline
DPPH	2,2-Diphenyl-1-Picrylhydrazyl
FTIR	Fourier Transform Infrared Spectroscopy
GRAS	Generally Recognized As Safe
HPH	High Pressure Homogenization
HSH	High Shear Homogenization
LM	Menthyl Laurate
MSG	Gliceryl Monostearate
MTS	(3-(4,5-Dimethylthiazol-2-Yl)-5-(3-Carboxymethoxyphenyl)-2-(4-Sulfophenyl)-2H-Tetrazolium)
NaCh	Sodium Cholate
NLC	Nanostructured Lipid Carriers
P188	Poloxamer 188
PC	Phosphatidylcholine
PdI	Polidispersity Index
PES	Phenazine Ethosulfate
PI	Propidium Iodide
Pip	Piperine
RMN	Nuclear Magnetic Resonance

RTCA	Real-Time Cell Analysis
TEM	Transmission Electronic Microscopy
TW20	Tween 20
UA	Thistle Oil
UC	Cocoa Butter
US	Sage Oil
Zave	Average Diameter

LIST OF FIGURES

FigureE 1: TLC analysis of the extract in chloroform (A) and isopropanol (B)	24
Figura 2: FTIR spectrum of isolated piperine	24
Figure 3: Mean diameter values obtained from DLS analysis of NLC coated with BSA*.....	31
Figure 4: Fluorescent emission spectra of NLC-II-BSA-1/2/3/4 compared with NLC without BSA (NLC-II-BSA-0) and BSA.....	32
Figure 5: STEM images of NLC-III-Pip-BSA-3 showing BSA corona formation on the surface of NLC particles (A-C); STEM images of NLC-III-BSA-0 showing spherical morphology and diameter according to DLS analysis (D,E)	32
Figure 6: Fluorescence emission spectra of NLC-Pip-BSA.....	33
Figure 7: Comparative release profile of Piperine from NLC with/without BSA coating.....	34
Figure 8: LoVo cell viability	35
Figure 9: Apoptosis in LoVo cells (A); MCF-7 cells (B);	36
Figure 10: ABTS●+ radical cation scavenging activity by	40
NLC-I- and -II- SambucusN with and without BSA.....	40
Figura 11: Efectul NLC convenționale și hibride asupra celulelor tumorale LoVo, după 48 de ore.....	41

LIST OF TABLES

Tabel 1: Piperine full NMR assignments.....	25
Tabelul 2: Menthyl laurate full NMR assignments	26
Tabel 3: Free-NLC fomultions (without encapsulated active ingredient)	27
Tabel 4: NLC formulations studied for their potential use in capturing the extract of <i>Sambucus nigra</i>	28
Tabel 5: Composition of nanostructured lipid transporter samples	30
Tabel 6: Proposed formulations for the encapsulation of <i>Sambucus nigra</i> extract	38

INTRODUCTION

Vegetal resources containing important fractions of polyphenols, flavonoids, alkaloids, terpenes, etc. represent a vast and as yet underexploited potential for health-related benefits. Mixtures of phytochemicals from different plant extracts are bioactive sources with a wide range of physiological and pharmacological activities. Owing to these bioactives, phytochemicals are known as traditional remedies with therapeutic efficacy for different types of ailments. Their medicinal potential is increasingly reported in the literature, e.g. for cardiologic disorders, diabetes and metabolic dysfunctions. The phytochemicals may exhibit antidepressant action, antioxidant activity but also a notable activity to halt and inhibit tumors located in certain areas of the body. The main bioactivity of polyphenolic extracts is related to their ability to scavenge free radicals and prevent lipid peroxidation, which significantly influence their health-promoting properties. Antioxidant activity helps to mitigate the damage caused by oxidative damage, the latter of which is known to be closely correlated with the development of several diseases, including cancer. Cancer is a complex and multifaceted disease that remains, despite advances in treatment, one of the leading causes of death. It is estimated that one in six deaths worldwide is caused by a cancer-related disease. Methods of treating cancer are varied and include surgery, chemotherapy, radiotherapy, and developing methods such as immunotherapy and hormonal treatment. However, the treatment of tumor diseases often faces challenges such as drug resistance, systemic toxicity and low efficacy of the therapeutic agent due to poor cell selectivity.

To overcome these difficulties, **drug delivery systems (DDS)** have emerged as a promising approach to traditional therapeutic agents [1]. These delivery systems have the potential to enhance the efficacy of drug treatment by improving drug biodistribution and pharmacokinetics, thereby reducing side effects and increasing drug concentration in the target tissue [2]. Depending on how they target cancerous tissue, DDSs can operate either by a passive or an active mechanism. Passive targeting involves the accumulation of DDS in tumors due to the physical and physiological characteristics of this tissue type. Although often used in the field of nanomedicine, the main drawback of this mechanism is the lack of specificity tumor cells vs. healthy cells [3,4]. On the other hand, active targeting involves decorating the surface of the transporters with specific ligands that can bind to receptors overexpressed on cancer cells.

This approach improves treatment specificity and drug delivery efficiency by transporting the active principle especially to tumor tissues. In addition, a reduction in systemic toxicity and adverse effects also occurs [5].

Among the different DDS, lipid systems are increasingly being studied in the pharmaceutical field, particularly for their ability to increase the bioavailability of drugs with low water solubility. The versatility of lipid formulations allows the synthesis of systems that can be tailored to specific medical indications, different routes of administration, as well as to requirements related to efficacy, stability and toxicity [6]. Among DDS systems, **Nanostructured Lipid Carriers (NLCs)** are a class of lipid nanoparticles, first described in 1999 [7], which have demonstrated increased adaptability and efficiency in the delivery of different pharmaceutical active ingredients. NLCs are formed from a mixture of solid and liquid lipids, stabilized with a surfactant coating, which confers a high loading capacity of the active ingredients. In addition, due to the carefully selected composition of the lipid core, the stability and controlled release capacity of the encapsulated active ingredients are enhanced. Moreover, biocompatibility and biodegradability are further added to these properties, as nanosystems are usually made of GRAS (“Generally Recognized as Safe”) materials [8].

In addition to these considerations, decorating NLC-type lipid systems with biopolymers such as serum albumin may be an **essential approach to construct optimized nanoplatfroms** to enhance the effects of phytochemical cancer therapy [9]. **Albumin** is the main plasma protein, previously used in obtaining DDS, due to its non-toxicity and non-immunogenicity. It has the ability to bind to specific receptors, such as GP60 and SPARC, overexpressed on the surface of tumor cells [10]. As such, by associating NLC with serum albumin (through non-covalent assembly, electrostatic interactions and hydrogen bonding), nanohybrid systems are obtained, which simultaneously harness the advantages of lipid nanoparticles in drug delivery with the tumor-targeting capabilities of albumin.

Considering all the above, **this doctoral thesis** addresses a new modality for the targeted delivery of phytochemicals using **NLC systems decorated with bovine serum albumin (BSA)**. A novel delivery platform consisting of BSA-coated NLCs (preparations with mixtures of vegetal oils and menthyl esters) **loaded with different bioactive phytochemicals** (e.g. *Piperine*, extracted from black pepper; polyphenol-enriched phytochemical mixture from *Sambucus nigra* extract) was considered for enhanced cellular internalization in different categories of tumor cells. The encapsulation of phytochemical active principles in hybrid nanocarriers is intended to improve the bioavailability of plant active principles while protecting them against degradation that may occur during gastrointestinal metabolism and

amplifying their potentially therapeutic effects. To the best of our knowledge, there are no studies in the literature addressing the coating of NLC-phytochemical plant principles with bovine serum albumin. Therefore, **the aim of this doctoral research** was to **evaluate the targeted effect of NLC-Phytochemical-BSA and untargeted NLC-Phytochemical-BSA on viability, proliferation, levels of cell cycle damage and apoptosis** in colon (LoVo), breast (MCF-7) and ovarian (SKOV-3) adenocarcinoma cell lines.). Suppression of tumor cells by NLC-Phytochemicals and the BSA-coated NLC-Phytochemicals hybrid delivery system was analyzed in **comparison with two well-known cytostatic drugs**, Cisplatin and Doxorubicin (DOX). No research has been identified in the literature that evaluated, analyzed and compared the cytotoxic action of a potential antitumor phytochemical versus conventional chemotherapeutic drugs (e.g. cisplatin, doxorubicin)

The PhD thesis entitled “**Hybrid lipid nanocarriers containing different plant active principles with antitumor potential**” contains 10 chapters, divided into two parts, bibliographical research and original contributions.

PART I - LITERATURE SURVEY aims to provide a comprehensive review of the existing literature regarding the characteristics and ability of NLC to present a relevant potential in the treatment of oncologic conditions. This literature review includes four chapters:

- **Chapter I** begins with a brief overview of drug delivery systems. Concepts of general characterization of the main lipid systems are covered, as well as methods of their delivery. Key features integrated in selected studies exploring the antitumor potential of NLCs conclude this first literature chapter.
- **Chapter II** makes the transition to NLC systems, i.e. those formulations of nanostructured lipid nanocarriers that present a non-uniform lipid core (adaptable for the integration of lipophilic active substances) and whose surface can be modified with different targeting molecules, so that improved therapeutic efficacy can be achieved, especially in the field of oncologic treatments. Thus, starting from the characteristics of cancer cells, the targeting mechanisms of tumor tissues (passive and active) are explained. At the end of the chapter, literature studies are described in which NLC systems are functionalized with the aim of targeting cancer cells more efficiently
- **Chapter III** is devoted to the in-depth knowledge of the structure and properties of the BSA protein, which due to its structural, biological and chemical characteristics can be considered an effective tumor cell targeting ligand. In support of this idea, a number of

recent scientific studies are presented in which various chemotherapeutic agents are encapsulated in albumin nanoparticles, or in other carrier systems that are surface functionalized with BSA.

- In **Chapter IV** the main aspects related to the active principles (piperine and polyphenolic extract of *Sambucus nigra*) encapsulated in the NLC systems described in this thesis are presented. The chapter contains information related to the sources of obtaining, chemical composition and biological activity.

PART II - ORIGINAL CONTRIBUTIONS initially introduces the research objectives, then continues with the development of original contributions in the field of **obtaining, characterization and applications of hybrid NLC** systems encapsulating different active principles of plant origin: i). **piperine** - a lipophilic active principle with known antitumor effect, but whose applicability is seriously affected by its insolubility in water; ii). **polyphenolic extract of *Sambucus nigra*** - an active mixture of hydrophilic principles with multiple biological benefits (e.g. antioxidant activity, anti-inflammatory effect, antitumor action, etc.), which is also limited in its use due to its thermal lability, but especially to the biological environment (it undergoes degradation during primary metabolism).

- **Chapter V** presents the raw materials, synthetic methods and analytical techniques used in the chapters related to the synthesis and characterization of NLC systems.
- **Chapter VI** presents studies on the obtaining of raw materials to be subsequently used in the synthesis of hybrid nanocarriers. Thus, this chapter describes the isolation of piperine, the active principle in the NLC systems described in Chapter VIII, from black peppercorns and the synthesis of menthyl laurate, a component of the lipid phase used in the formulation of the NLC systems obtained in Chapter IX.
- **Chapter VII** details preliminary optimization studies of the lipid-surfactant composition in order to obtain aqueous dispersions of NLCs exhibiting suitable structural characteristics for establishing effective interactions with the BSA biopolymer.
- Chapter VIII includes the original results on the development and characterization of conventional NLCs and hybrid NLCs (with high content of **cocoa butter** and **thistle oil**) encapsulating piperine. The chapter addresses a dimensional, morphostructural and spectroscopic characterization of the synthesized hybrid systems. The therapeutic activity of these nanocarriers is evaluated by *in vitro* antioxidant activity assays,

controlled release studies, preceded by cytotoxicity evaluation on three cancer cell lines: LoVo (colon cancer), SKOV-3 (ovarian cancer) and MCF-7 (breast cancer).

- **Chapter IX** describes the main results obtained from the synthesis of hybrid NLCs by significantly modifying the composition of the lipid core consisting of **a mixture of coconut butter, sage oil and menthyl laurate**. The obtained hybrid nanocarrier systems were tested for their ability to co-opt a complex mixture of polyphenolic phytochemicals present in *Sambucus nigra* extract. Following structural and physicochemical characterization, the anti-tumor properties are determined in vitro by cytotoxicity assays, apoptosis analysis on LoVo, SKOV-3 and MCF-7 cell lines and cell cycle modification.
- The **last chapter (X)** integrates the final conclusions and the main original contributions brought by the thematic addressed in this PhD thesis.

The results of the original research were disseminated through the publication of **4 articles in ISI journals** (3 in international journals and one national), which cumulate an impact factor FIC = 14.4. Some of the results were also presented at an international conference (as oral presentation) and at a national conference (as poster).

II. ORIGINAL CONTRIBUTIONS

AIM AND OBJECTIVES

Despite the substantial development of NLCs, the adverse effects of chemotherapeutic drugs, lack of localization ability to cancer cells and detected chemoresistance have proved to be the main challenges in the efficiency of the chemotherapy process. As such, **the association of NLC-type lipid nanocarriers with albumin biopolymer** in an efficient and optimized manner to construct so-called “hybrid nanoplatforms for bioactive phytochemicals” to enhance tumor cell targeting effects is a novel approach with a positive impact on **improving** oral bioavailability and enhancing antitumor efficacy. In addition, **phytochemical mixtures** represent valuable sources of bioactive principles that may exhibit synergistic effects.

Based on the concept that tumor cells can be targeted by altering the surface of nanostructured delivery systems and in view of the growing interest in health-promoting plant active substances (phytochemicals), **the present PhD thesis AIMED** to investigate the adaptability of **conventional (NLC) as well as hybrid lipid nanocarriers** (lipid-polymeric, BSA-coated NLC, NLC-BSA) **to co-opt different bioactive principles** to improve the penetration and targeting of some tumor cells and enhance the efficacy of antitumor therapy. The bioactive principles selected in the present PhD thesis are: **piperine** - an alkaloid extracted from black pepper, with multiple pharmacological benefits, which are however limited due to its properties and the way it is metabolized, and ***Sambucus nigra* extract** - a phytochemical mixture rich in bioactive compounds, which may be an alternative to traditional oncological therapy.

In order to support the hypotheses of the experimental work and to achieve the aim pursued in this doctoral thesis, several **OBJECTIVES** have been followed, which were:

- I. Isolation and characterization of a bioactive principle from black pepper, *Piperine*. Synthesis and characterization of *menthyl laurate*.
- II. Optimization of obtaining conventional NLC and polymer decorated NLC; characterization and monitoring of different formulation parameters, stability and biopolymer concentration.
- III. **Obtaining and morpho-structural characterization of conventional NLCs and BSA-coated NLCs** loaded with piperine and black elderberry/*SambucusN* extract

(NLC-Pip, NLC-Pip-BSA, NLC-SambucusN, NLC-SambucusN-BSA), respectively, in terms of particle size, morphology, Zeta potential, phytochemical encapsulation efficiency, FTIR and fluorescence spectroscopy.

- IV. Evaluation of some biological activities by *in vitro* determination** of specific properties such as antioxidant activity, release profile, cytotoxicity, influence on cell cycle, etc. Comparative attribution of the antitumor effect of different categories of NLCs (cell viability, proliferation, level of cell cycle damage and apoptosis) was achieved by using tumor cell lines, e.g. MCF-7 breast cancer cells, LoVo colon and SKOV-3 ovarian adenocarcinoma cells, and their efficacy was compared with conventional chemotherapeutic drugs, Doxorubicin and Cisplatin. To the best of our knowledge, **this study is the first to explore the combinatorial potential of *Sambucus Nigra* and albumin-decorated nanostructured lipid nanocarriers as novel durable nanocarriers to support targeted anti-tumor therapy, especially for synergistic colon, ovarian and/or breast therapy.**

CHAPTER V

METHODS AND MATERIALS

5.1. Materials and reagents

The following compounds and raw materials were used to obtain free NLC systems (without active ingredient) and those loaded with various active ingredients, as well as those coated with BSA:

- **Solid lipids:** Glyceryl monostearate (GMS), cocoa butter, coconut butter. GMS was purchased from Cognis GmbH (Monheim am Rhein). Cocoa butter and coconut butter were purchased from Plafar, manufactured by Green Sense.
- **Liquid lipids:** Thistle oil (UA), sage oil (US), menthyl laurate. The oils were purchased from Texron Plimon S.L.U. (Barcelona, Spain). Menthyl laurate was synthesized and characterized in the laboratory (see Chapter VI).
- **Surfactants:** Sodium dioctyl sulfosuccinate (AOT), lecithin (PC), Tween 20 (TW20), sodium cholate (NaCh), Poloxamer 188 (P188). TW20 was supplied by Merck (Darmstadt, Germany). NaCh, P188, and AOT were purchased from Sigma Aldrich Chemie GmbH (Munich, Germany). Lecithin was supplied by Alfa Aesar (Karlsruhe, Germany).
- **Surface modifiers:** Bovine serum albumin (BSA) purchased from Sigma Aldrich Chemie GmbH (Munich, Germany).
- **Active ingredients:** piperine, *Sambucus nigra* extract. Piperine was extracted and characterized in the laboratory (see Chapter VI). *Sambucus nigra* extract was supplied by A.C. Helcor, Baia Mare, Romania.

During the physicochemical characterization of the obtained NLCs, the following reagents and solvents were used: sodium chloride, ethanol, 2,2-diphenyl-1-picrylhydrazyl (DPPH), Folin–Ciocâlteu reagent, gallic acid, 2,2'-azino-bis(3-ethylbenzothiazoline-6-sulfonic acid) (ABTS), dimethyl sulfoxide (DMSO), and potassium persulfate — all purchased from Sigma-Aldrich Chemie GmbH.

Tumor cell lines were obtained from the American Type Culture Collection (ATCC). The following reagents were used during *in vitro* biological testing: DOX, DMEM culture medium (Dulbecco's Modified Eagle's Medium), cisplatin (Cis-Pt), L-glutamine (Glu), phosphate-buffered saline (PBS)/1 mM EDTA, penicillin (100 units/mL), fetal bovine serum

(FBS), propidium iodide (PI), and RNase A — all purchased from Sigma-Aldrich (St. Louis, MO, USA).

5.2. Synthesis of hybrid NLC

For the synthesis of NLC systems, modified high-pressure homogenization (HPH) was used. In outline, the molten lipid phase (containing the mixture of lipids and lipophilic active ingredients) and the aqueous phase (containing surfactants and hydrophilic active ingredients) were mixed at the same temperature (72 °C). The resulting pre-emulsion was maintained under vigorous stirring at 72 °C for 20 minutes, then subjected to a high shear homogenization (HSH) step and then a HPH step for 3 minutes and 17 seconds at 500 bar. To remove water and obtain NLC in solid form, the previously obtained nanoemulsions were subjected to a freeze-drying process using an Alpha 1-2 LD Freeze Dry System, Germany, after freezing for 24 hours at -25 °C. The freeze-drying parameters were 55 °C and 0.05 mbar for 55 hours.

To obtain hybrid systems, i.e., those systems where the surface of the nanostructured lipid carriers is coated with bovine serum albumin, a volume of dispersion obtained after HPH was mixed with a volume of BSA solution of varying concentrations under agitation, then stirred until reaching room temperature.

5.3. Structural, morphological, and functional characterization of NLC systems

The synthesized NLC systems were characterized in terms of their structure, morphology, and biological activity. Thus, the parameters that influence particle size and colloidal stability (DLS and Zeta potential) and particle morphology (TEM) were determined. In addition, the interactions between the different components of the systems were evaluated using spectroscopic methods. The functionality of the obtained systems was assessed by *in vitro* release tests, by measuring antioxidant activity, and by tests on three types of tumor cells (colon – LoVo, breast – MCF-7, and ovarian – SKOV-3).

5.3.1. Determination of Particle Size and Size Distribution

The average particle diameter (Z_{ave}) and polydispersity index (PdI) were determined using a Zetasizer ZS90 instrument (Malvern Instruments Inc., Worcestershire, UK) equipped with a solid-state laser ($\lambda = 690$ nm), recording at a scattering angle of 90° and a temperature of 25 ± 0.1 °C. To minimize multiple scattering effects, the samples were diluted to ensure optimal signal quality. Particle size was determined by averaging the intensity distributions obtained from three individual measurements.

5.3.2. Determination of Zeta Potential

Zeta potential was measured using a Zetasizer ZS90 instrument (Malvern Instruments Inc., Worcestershire, UK) with specialized capillary cells. The dispersions were diluted first with distilled water, then with 0.9% NaCl solution to achieve a conductivity of 50 $\mu\text{S}/\text{cm}$, ensuring appropriate measurement conditions. The surface charge of the systems was calculated using the Helmholtz–Smoluchowski equation (Equation 5.1), where μ_e is the electrophoretic mobility, η is the viscosity of the medium, and ϵ is the dielectric constant.

$$\zeta = \frac{\mu_e \cdot \eta}{\epsilon} \quad (5.1)$$

5.3.3. Particle morphology analysis

In this thesis, several NLC and hybrid NLC systems that showed optimal characteristics in terms of structure and properties were selected for microscopic analysis, using a Hitachi HD 2700 device that combines scanning and transmission microscopy. Sample preparation consisted of diluting the dispersions with distilled water and then depositing them on standard TEM copper grids with a thin carbon coating, and the studies were performed using the device in TEM mode, as well as in Z contrast or HAADF (High Angle Annular Dark Field Mode) mode.

5.3.4. Fourier transform infrared spectroscopy (FTIR)

During the studies described in this thesis, the IR spectra of the lyophilized carriers were recorded with a Bruker Vertex 70 spectrometer, equipped with a horizontal attenuated reflection (ATR) device and diamond crystal, on a spectral window of 4000-400 cm^{-1} .

5.3.5. Fluorescence spectroscopy

Fluorescence spectra were recorded using a Jasco FP-650 spectrofluorometer (Tokyo, Japan) equipped with a microcomputer for data recording. The samples were excited with radiation having a wavelength of 285 nm.

5.3.6. Determination of the Encapsulation Efficiency of Active Ingredients by UV-Vis Spectroscopy

In this study, the encapsulation efficiencies of the active phytochemical compounds—piperine and *Sambucus nigra* extract—were determined using UV-Vis spectroscopy. A Jasco V670 UV-Vis spectrophotometer (Tokyo, Japan) was used for the measurements.

Determination of Piperine Encapsulation Efficiency

The quantification of piperine by UV-Vis spectroscopy was based on generating a calibration curve within the concentration range of 1–10 µg/mL. Standard solutions (of known concentrations) were measured at the maximum absorption wavelength of $\lambda = 342$ nm, using ethanol as the solvent, with a blank sample containing only ethanol as reference.

The following procedure was applied to determine the encapsulated piperine in nanocarriers: 0.5 g of lyophilized NLC was dispersed in a minimal volume of ethanol (1 mL). The dispersion was centrifuged at 13000 rpm for 15 minutes using a Sigma 2K15 centrifuge (Osterode am Harz, Germany). The piperine content in the resulting supernatant was then quantified by UV-Vis spectroscopy, and its concentration was determined using the regression equation from the calibration curve. This concentration was subsequently converted into the corresponding mass of encapsulated piperine.

Determination of the Encapsulation Efficiency of *Sambucus nigra* Extract Using the Folin–Ciocâlteu Method

To experimentally determine the amount of polyphenols encapsulated in the NLC, a calibration curve was first established using gallic acid as a standard. A stock solution with a concentration of 200 mg/L was prepared in a 100 mL volumetric flask, and working standard solutions ranging from 10 to 100 mg/L were obtained by serial dilution. For the reaction with the Folin–Ciocâlteu (F-C) reagent, 0.5 mL of gallic acid solution and 0.5 mL of 10% F-C reagent were mixed in 5 mL volumetric flasks and homogenized for 4 minutes. Next, 4 mL of 7.5% Na₂CO₃ solution was added. The resulting solutions were kept in the dark for one hour to allow the reaction to proceed to completion. Absorbance was then measured using a Jasco V-650 spectrophotometer at $\lambda = 765$ nm.

The optimized experimental protocol for determining polyphenol content in the NLC consisted of the following steps:

- ✓ Suspension of 0.15 g of lyophilized NLC in 1 mL of distilled water, with gentle stirring
- ✓ Centrifugation for 5 minutes at 15000 rpm
- ✓ Collection of 0.5 mL of supernatant and treatment with 2.5 mL of 10% F-C reagent, followed by 2 minutes of stirring
- ✓ Addition of 2 mL of 7.5% Na₂CO₃ solution
- ✓ Incubation in the dark for 1 hour to complete the reaction
- ✓ Absorbance measurement at $\lambda = 765$ nm

5.3.6. In Vitro Evaluation of Free Radical Scavenging Capacity

To assess the *in vitro* antioxidant activity of the NLCs synthesized in this study, two spectrophotometric methods were employed: DPPH and ABTS assays.

DPPH assay

This method involves mixing an ethanolic solution of DPPH (40 µg/mL) with an ethanolic solution of NLC (10 mg/mL), followed by a 30-minute incubation. The final solution was analyzed using a Jasco V-650 spectrophotometer at a wavelength of $\lambda = 517$ nm. The DPPH radical scavenging capacity was calculated using Equation 5.8, where A_p represents the absorbance of the test sample and A_M the absorbance of the control. Control samples were prepared by replacing the NLC solution with ethanol.

$$Inhb(\%) = \left(1 - \frac{A_p}{A_M}\right) \cdot 100 \quad (5.8)$$

ABTS assay

This method is based on the colorimetric change resulting from the quenching of ABTS \bullet^+ radicals, which can be monitored spectrophotometrically at $\lambda = 734$ nm. The ABTS \bullet^+ radicals were generated by mixing aqueous solutions of 7 mM ABTS and 2.45 mM K₂S₂O₈ in a 1:1 volumetric ratio. To complete the reaction, the mixture was stored in the refrigerator overnight, then diluted with ethanol to achieve an absorbance of 0.7 at $\lambda = 734$ nm (designated as ABTS_N). To evaluate the antioxidant activity of the NLCs, an ethanolic solution of lyophilized NLC (5 mg/mL) was mixed with an equal volume of ABTS_N solution. After 4 minutes of stirring, absorbance was measured at $\lambda = 734$ nm using a Jasco V-650 spectrophotometer.

5.3.7. In vitro evaluation of the active ingredient release profile

The *in vitro* release profile of piperine was evaluated using the dialysis bag method. Specifically, 5 mL of NLC dispersion was sealed in a dialysis bag (MW = 12–14 kDa) and placed in a vessel containing 50 mL of receiving medium (ethanol:water, 1:1), under continuous magnetic stirring at 37 °C and 300 rpm (Figure 5.19B). The release was monitored over a period of 5 hours by periodically collecting 0.5 mL samples from the receiving medium, which were analyzed by UV-Vis spectroscopy to determine the concentration of piperine. After each sampling, the withdrawn volume was replaced with an equal volume (0.5 mL) of fresh receiving medium.

5.3.8. *In vitro* cytotoxicity analysis by MTS assay

For the *in vitro* determinations, 96-well flat-bottom plates (Thermo Scientific, Waltham, MA, USA) and the CellTiter 96 Aqueous One Solution Cell Proliferation Assay kit (Promega, Madison, WI, USA) were used. Each well was seeded with 10^4 cells in 100 μ L of medium and incubated for 24 hours, after which the supernatant was removed. The cells were then treated for 24 or 48 hours with increasing concentrations of NLC. At the end of the incubation period, 20 μ L of the staining reagent containing MTS and PES (phenazine ethosulfate) were added to each well. The plates were further incubated for 4 hours at 37 °C with gentle shaking every 15 minutes. The reduction of the tetrazolium compound to formazan was measured spectrophotometrically at $\lambda = 492$ nm using a Dynex well plate reader (Dynex Technologies MRS, Chantilly, VA, USA).

Cell viability was calculated relative to untreated control cells (considered 100% viable) using equation 5.9, where:

- $Abs_{treated\ cells}$ = absorbance of treated cells
- $Abs_{untreated\ cells}$ = absorbance of untreated cells
- $Abs_{culture\ medium}$ = absorbance of the culture medium

$$Cell\ viability, \% = \frac{Abs_{treated\ cells} - Abs_{culture\ medium}}{Abs_{untreated\ cells} - Abs_{culture\ medium}} \cdot 100 \quad (5.9)$$

5.3.9. Real-time cytotoxicity analysis (RTCA method)

Cells were seeded in 16-well E-Plates (ACEA Biosciences, USA) containing 100 μ L of culture medium composed of DMEM supplemented with 2 mM L-glutamine and 10% fetal bovine serum. Growth curves were recorded automatically in real time using the xCELLigence system until a Cell Index (CI) above 1 was reached (typically after 24 hours). Subsequently, the NLC formulations were added, and the curves were monitored using RTCA software version 2.1.2. By tracking changes in the CI over time, a drug-specific profile can be generated, reflecting the biological mechanism of action of the active ingredient.

5.3.10. Apoptosis analysis by flow cytometry

In the studies presented, the Annexin V-FITC Apoptosis Detection Kit (Becton Dickinson Biosciences) was used. Briefly, 10^5 cells were suspended in 100 μ L of buffer solution in a tube and stained simultaneously in the dark with 5 μ L Annexin V-FITC and 5 μ L propidium iodide (PI) for 15 minutes. After staining, 400 μ L of buffer was added to optimize the cell concentration for flow cytometric analysis. Apoptotic events were quantified using a FACS

Canto II flow cytometer (Becton Dickinson Immunocytometry System, Mountain View, CA, USA). Using DIVA software version 6.2, viable cells (FITC-negative, PI-negative) were distinguished from necrotic cells (FITC-positive, PI-positive) and cells in early apoptosis (FITC-positive, PI-negative) versus late apoptosis.

5.3.11. Cell cycle analysis by flow cytometry

For cell cycle analysis, 10^6 ethanol-fixed cells were washed with PBS and suspended in 350 μ L PBS. Then, 50 μ L of 10 mg/mL RNase A solution was added, and the cells were incubated at 37 °C for 10 minutes. Next, 100 μ L of 100 mg/mL propidium iodide (PI) solution was added and incubated for another 10 minutes at 37 °C. Samples were analyzed using the FACS Canto II cytometer, and data analysis was performed with ModFit software.

5.4. Isolation and characterization of piperine from black pepper berries

The extraction apparatus consisted of a round-bottom flask equipped with a Thielepappe extractor, heating, and magnetic stirring. An ascending condenser was mounted above the extractor. 300 mL of extraction solvent was placed in the round-bottom flask, while 60 g of freshly ground black pepper was loaded into the extractor on a layer of cotton wool. The solvent was heated to reflux for 6 hours, and the flow rate through the extractor was adjusted to ensure that the pepper layer remained fully immersed in the solvent at all times. At the end of extraction, the alcoholic extract was evaporated to dryness. The residue obtained was dissolved in 20 mL of 0.1 g/mL KOH solution in isopropanol. Piperine was precipitated from this solution by adding distilled water. After filtration, piperine was purified by recrystallization from isopropanol.

TLC analysis was performed by spotting a small amount of sample onto silica gel plates and eluting with a toluene:ethyl acetate mixture (7:3, v/v).

The melting point of piperine was determined by thermoanalysis using a Polytherm A microscope (a microscope equipped with a Boëtius hot plate) connected to a temperature-controlled heating device from Wagner & Munz, Munich, Germany.

FTIR spectra were recorded using a Bruker VERTEX 70 spectrometer.

NMR spectra were acquired on a Bruker AVANCE III HD 600 MHz spectrometer (Bruker, Rheinstetten, Germany) operating at 600.12 MHz for ^1H , equipped with a 5 mm z-gradient probe with multinuclear inverse detection (BBI).

5.5. Synthesis and characterisation of menthyl laurate

The synthesis of menthyl laurate (the menthyl ester of lauric acid) was carried out following a modified Neises method [1]. 0.01 mol of lauric acid and 0.001 mol of N,N-dimethylaminopyridine (DMAP) were dissolved in 25 mL of methylene chloride. Then, 0.01 mol of menthol was added, and the solution was cooled to 0 °C. Subsequently, 0.01 mol of N,N-dicyclohexylcarbodiimide (DCC) was added, and the mixture was stirred at 0 °C for 5 minutes and then at room temperature for 3 hours. The precipitate was filtered off, and the supernatant was evaporated under vacuum (10 mmHg) to yield a residue. The residue was dissolved in a small volume of methylene chloride, and any further precipitate formed was removed by filtration. The solution was washed twice with 25 mL portions of 0.5 N hydrochloric acid and then dried under reduced pressure. The crude product was purified by silica gel column chromatography. Elution was performed using a gradient of ethyl ether (EE) and ethyl acetate (EP). Evaporation of the solvent from the fraction eluted with a 1:9 EE:EP mixture yielded the pure analytical compound.

TLC analyses were conducted by eluting with EE:EP = 1:3. Plates were developed either by immersion in bromocresol green solution or in phosphotungstic acid alcoholic solution, followed by heating on a hot plate until black spots appeared.

Spectroscopic analyses were performed using the same methods as for piperine.

CHAPTER VI

Extraction of Piperine and synthesis of Menthyl Laurate

This chapter presents the preparation of raw materials that were later used for synthesizing NLC systems. Piperine was used as the active ingredient in the formulations described in Chapter VII, while menthyl laurate was part of the lipid phase in the systems described in Chapter VIII.

6.1. Extraction of Piperine from Black Pepper Berries

Piperine, the main alkaloid with biological properties found in *Piper nigrum* and *Piper longum* plants, was obtained by a solid-liquid extraction process. Instead of the classical Soxhlet method, a Thielepappe extractor was used. The design of this apparatus allows continuous flow of fresh solvent through the substrate, enabling faster extraction while using less solvent. The main steps of the process include: grinding the pepper berries, performing the extraction itself, concentrating the extract, saponifying acidic impurities, precipitating piperine as a fine white-yellow solid, and recrystallizing it in pure form from isopropyl alcohol as crystals with a melting point of 127–128 °C.

Regarding solvent selection, chloroform and isopropyl alcohol were tested. These two solvents show a major difference in selectivity. Figure 5A shows that although, according to the literature [2] piperine has high solubility in chloroform (588 mg/mL), its selectivity during extraction is low, as evidenced by TLC analysis of the extract showing five main compounds. On the other hand, isopropanol is a very selective solvent, from which piperine was easily isolated with a yield of about 3% (compared to the Soxhlet method, where the yield was below 1% for the same extraction time)

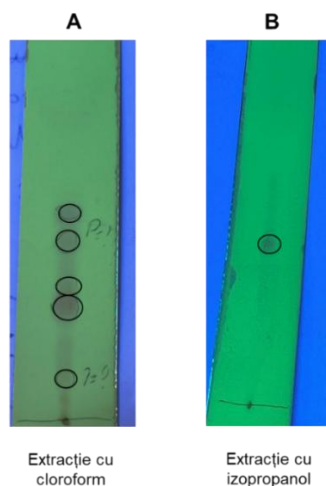


Figure 1: TLC analysis of the extract in chloroform (A) and isopropanol (B)

6.2. Spectroscopic analysis of Piperine

The structure and purity of the piperine crystals were confirmed by infrared spectroscopy and nuclear magnetic resonance spectroscopy.

The ATR-FTIR spectrum (Figure 2) highlights the presence of all characteristic bands of the piperine structure (for example, the bands at 1579 cm^{-1} and 1522 cm^{-1} confirm the presence of the conjugated double bond system).

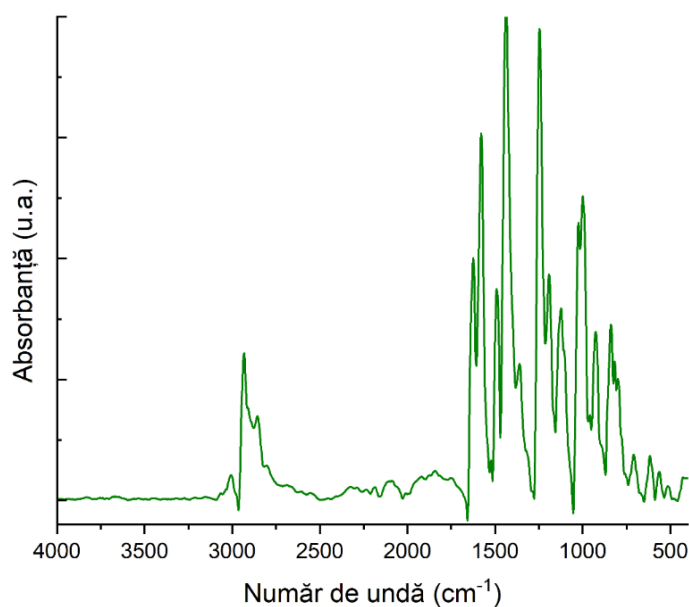


Figura 2: FTIR spectrum of isolated piperine

For a comprehensive analysis, classic NMR spectra of the types ^1H -NMR and ^{13}C -NMR were recorded, as well as two-dimensional spectra such as COSY (**H**omonuclear **C**orrelation

Spectroscopy), HMQC (Heteronuclear Multiple Quantum Coherence), and HMBC (Heteronuclear Multiple Bond Correlation) to achieve the most precise assignment of each signal from the one-dimensional spectra.

The ^1H -NMR spectrum contains three distinct regions, corresponding to the piperine substructures they belong to (benzodioxole, piperidine, or the diene system). The carbon spectrum was consistent with the molecular formula of piperine and allowed for the identification of the amide carbon. Additionally, the 2-D techniques enabled the exact assignment of each signal. Table 1 presents a summary of the assignments made.

Tabel 1: Piperine full NMR assignments

Atom #	^{13}C ($\delta[\text{ppm}]$)	^1H ($\delta[\text{ppm}]$, m, J[Hz], I)	COSY	HMBC
1	165,39	-	-	4, 9
2	148,15	-	-	8, 10, 11
3	148,07	-	-	
6	130,99	-	-	10, 5/7
4	142,43	7,39 (ddd, $J = 14,7$; 9,2; 1,1 Hz, 1H)	5/7, 9	5/7
5	138,17	6,75 – 6,68 (m, 2H)	4	4, 8, 11
7	125,33			4, 8, 9
8	122,45	6,88 (dd, $J = 8,1$; 1,7 Hz, 1H)	10	7, 10, 11
9	120,03	6,43 (d, $J = 14,6$ Hz, 1H)	4	4, 5
10	108,44	6,77 (d, $J = 8,0$ Hz, 1H)	8	8, 11
11	105,63	6,97 (d, $J = 1,7$ Hz, 1H)	-	7, 8
12	101,23	5,96 (s, 2H)	-	-
13/14	46,87/43,20	3,52 (br. s, 2H)/3,63 (br. s, 2H)	15/16	15, 16, 17
15/16	26,70/25,59	1,61 – 1,54 (m, 4H)	13/14	13, 14, 17
17	24,62	1,69 – 1,62 (m, 2H) /	13/14	13, 14, 15, 16

6.3. Synthesis and characterization of menthyl laurate

The synthesis of menthyl laurate was performed using Steglich esterification, which uses dicyclohexylcarbodiimide (DCC) as a coupling agent and N,N-dimethylaminopyridine (DMAP) as a catalyst, because this reaction takes place under milder conditions compared to classical Fischer esterification, which can lead to secondary reactions.

The setup consists of a round-bottom flask equipped with magnetic stirring and a septum. The procedure is equally simple, involving mixing the reactants initially at 0 °C and then at room temperature, followed by filtration, neutralization of the compounds, and finally column chromatography to obtain the pure ester. The synthesis proceeded with a yield of approximately 88%, and spectral analyses showed that a pure compound was obtained. Table 2 shows the assignments of the signals in the NMR spectra obtained through an analysis similar to that used for piperine.

Table 2: Menthyl laurate full NMR assignments

Atom #	¹³ C (δ[ppm])	¹ H (δ[ppm], m, J[Hz], I)	COSY
1	173,49	-	-
2	73,87	4,67 (td, <i>J</i> = 10,9, 4,4 Hz, 1H)	4e, 4a, 3
3	47,04	1,36 (tt, <i>J</i> = 11,9; 11,1; 3,5; 2,9 Hz, 1H)	2, 13a
4	40,97	a: 0,95 (q, <i>J</i> = 12,0 Hz, 1H)	4a, 4e, 8
		e: 2,03 – 1,93 (m, 1H)	2, 13e, 4a
5	34,78	2,27 (td, <i>J</i> = 7,3; 1,1 Hz, 2H)	12
6	34,30	a: 1,72 – 1,64 (m, 2H)	3, 6e, 13e
		e: 0,91 – 0,81 (m, 10H)	-
8	31,91	1,53 – 1,44 (m, 1H)	4a, 14
11	26,25	1,90 – 1,81 (m, 1H)	3, 16, 17
12	25,16	1,63 – 1,58 (m, 2H)	5
13	23,43	a: 1,05 (qd, <i>J</i> = 14,1; 12,5; 4,3 Hz, 1H)	13e, 6e, 6a, 3
		e: 1,72 – 1,64 (m, 2H)	3, 6e
14	22,68	0,91 – 0,81 (m, 10H)	-
16	20,76	0,91 – 0,81 (m, 10H)	-
17	16,29	0,75 (d, <i>J</i> = 7,0 Hz, 3H)	11, 16
18	14,11	0,91 – 0,81 (m, 10H)	-
7/9/10/15/ 18-21	31,38/29,61/29,60/29,49/29,34/29,2/ 29,14/22,03	1,33 – 1,22 (m, 16H)	-

Note: The notations *a* and *e* refer to hydrogen atoms in axial and equatorial positions, respectively..

CHAPTER VII

Studii preliminare de optimizare a compoziției NLC

According to the specialized literature [3,4], the selection of surfactants plays a crucial role in controlling particle size and ensuring the physical stability of the colloidal system. Thus, this chapter presents studies carried out to optimize the surfactant mixtures used in NLC formulations so that they exhibit characteristics leading to a colloidal dispersion with appropriate particle size, high stability, and efficient binding of BSA.

7.1. Optimization of NLC formulations for piperine encapsulation

To identify an optimal surfactant-to-lipid mixture composition capable of encapsulating piperine, four formulations were initially evaluated as shown in Table 3. These formulations were designed so that the mass ratio between solid and liquid lipids remained constant at 7:3, while the surfactant mixture accounted for 2% of the final formulation. Additionally, variations in the ratio among the three types of surfactants can be observed.

Tabel 3: Free-NLC fomultions (without encapsulated active ingredient)

Sample name	Lipid phase			Aqueous phase		
	MSG (g)	UC (g)	UA (g)	AOT (g)	PC (g)	TW20 (g)
NLC-surf.1	3,5	3,5	3	0,5	0,5	1
NLC-surf.2	3,5	3,5	3	0,7	0,3	1
NLC-surf.3	3,5	3,5	3	0,3	0,7	1
NLC-surf.4	3,5	3,5	3	0	0,3	1,7

The selection of optimal formulations was based on data obtained from DLS and electrophoretic potential analyses. For example, NLC-surf. 1 forms a stable dispersion with particle diameters of approximately 183 nm, relatively constant over time. On the other hand, NLC-surf. 2 results in a dispersion with larger particle sizes, which increase further over the course of a week, suggesting the onset of aggregation processes. This hypothesis is also supported by the Pdl value. Remarkable results were obtained for NLC-surf. 3, which proved to be one of the most stable formulations tested, thanks to its high PC content, which, according to the literature [5] improves the stability of the lipid core. Surprising results were also observed

for NLC-surf. 4, which, despite having a lower zeta potential than the other formulations, was the most uniform dispersion among all tested systems.

In conclusion, the composition of the surfactant mixture significantly influences the stability and characteristics of the NLC formulations. **NLC-surf. 3 and NLC-surf. 4 proved to be the most stable formulations due to optimized ratios of surfactants that effectively balance steric and electrostatic stabilization.** These two formulations were then subjected to BSA coating, with the experimental results described in Chapter VIII.

7.2. Optimization of NLC formulations for encapsulating the polyphenolic extract of *Sambucus nigra*

Following a methodology similar to that used for the systems tested for piperine encapsulation, four initial formulations were proposed for the encapsulation of the polyphenolic extract of *Sambucus nigra*, as shown in Table 4. The surfactant mixture mainly consisted of NaCh, TW20, and PC; however, in two of the formulations, a small amount of TW20 was replaced with P188, which, due to its structure, can induce additional steric hindrance and may have a synergistic effect in reducing particle size [6].

Tabel 4: NLC formulations studied for their potential use in capturing the extract of *Sambucus nigra*

Sample name	Lipid phase			Aqueous phase				C _{SI} * (mg/mL)
	MSG (g)	CB (g)	US (g)	NaCh (g)	PC (g)	TW20 (g)	P188 (g)	
NLC-1	3,5	3,5	3	0,2	0,3	2	-	3,8
NLC-2	3,5	3,5	3	0,3	0,7	1,5	-	7,7
NLC-3	3,5	3,5	3	0,2	0,3	1,7	0,3	3,8
NLC-4	3,5	3,5	3	0,3	0,7	1,35	0,15	7,7

* C_{SI} – concentration of ionic surfactants, relative to the final volume of the dispersion, 130 mL

The particle size analysis results show that formulations with a high concentration of ionic surfactants yield smaller particles, whose diameters remain stable even after two weeks of refrigeration. For example, NLC-2 particles measured 128 nm immediately after synthesis and 122 nm after two weeks. In contrast, formulations with a lower ionic surfactant content produce larger particles, which tend to increase in size over time; NLC-1 particles measured 165 nm initially and 175 nm after two weeks. These observations are supported by both Pdl

values and Zeta potentials, with NLC-2 and NLC-4 exhibiting higher absolute values compared to NLC-1 and NLC-3.

All four formulations were coated with BSA by mixing the dispersions with an aqueous BSA solution (40 mg/mL) in volume ratios of 3:1 and 1:1 (v/v), respectively. The results indicate that BSA binding to the NLC surface does not significantly affect particle size in suspension. However, Zeta potential values undergo substantial changes, showing a decrease in absolute value for most dispersions, attributable to partial neutralization of particle surface charges.

In conclusion, a 1:1 volume ratio between dispersion and BSA solution is optimal for forming a dense protein layer on the particle surface.

CHAPTER VIII

Novel Bovine Serum Albumin-Decorated–Nanostructured Lipid Carriers Able to Modulate Apoptosis and Cell-Cycle Response in Ovarian, Breast, and Colon Tumoral Cells

This chapter describes the development and testing of simple/hybrid nanostructured lipid nanocarriers in which piperine has been encapsulated. This topic is important because nanosystems for the delivery of this alkaloid allow the enhancement of phytopharmaceutical effects, which by administration in free form, are limited due to low water solubility, extensive first-passage effect and toxicity at high concentrations. The anti-tumor potential of piperine-loaded NLC (with and without BSA) was evaluated on the viability, proliferation and cell cycle influence of LoVo (colon cancer), MCF-7 (breast cancer) and SKOV-3 (ovarian cancer) cells, and compared with two well-known cytostatic drugs, cisplatin (Cis-Pt) and Doxorubicin (DOX).

8.1. Optimization of surfactant and albumin composition for new BSA -NLC formulations

Based on the results obtained in section 7.1, two formulations were proposed for BSA coating as shown in Table 5. Coating of NLC with BSA was performed by mixing an equal volume of NLC and aqueous BSA solution of different concentrations (between 1 and 20 mg/mL).

Tabel 5: Composition of nanostructured lipid transporter samples

Sample name	Lipid phase, g			Aqueous phase, g		
	MSG	UC	UA	AOT	PC	TW20
NLC-I	3,5	3,5	3	0	0,3	1,7
NLC-II	3,5	3,5	3	0,3	0,7	1

DLS analysis

Following the evaluation of the average diameter of the BSA-coated nanocarriers (Figure 3), a mass ratio of surfactant TW20:PC:AOT = 1:0.7:0.3 leads to the formation of particles with Zave ~ 150 nm, which does not vary significantly with increasing amount of

BSA. In terms of colloidal dispersion stability, all the synthesized systems exhibit values between -52 mV and -80 mV, with the remark that the series II formulations (containing TW20-PC-AOT) exhibit better dimensional and stability characteristics than the series I formulations.

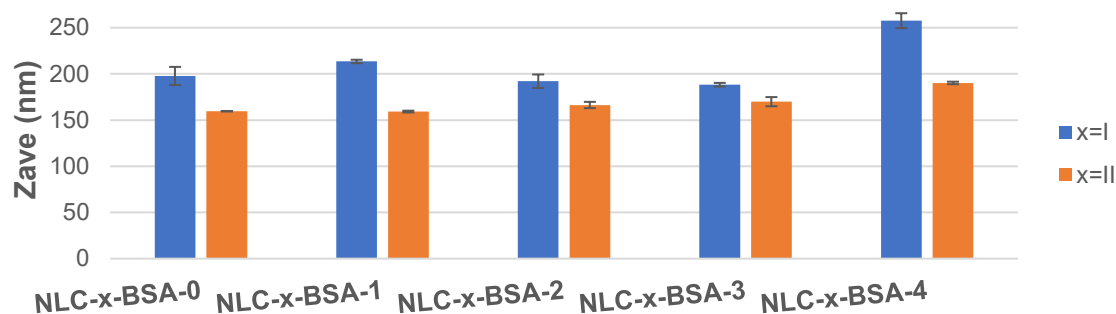


Figure 3: Mean diameter values obtained from DLS analysis of NLC coated with BSA*

*NLC-x-BSA-0 are NLCs without BSA

FTIR analysis

All solid NLC spectra exhibited similar characteristic bands for both BSA and the fundamental components of NLC. It could be observed that the intensity of the BSA bands increased with increasing concentration, simultaneously with the enhancement of the vibrational bands at $\sim 3300\text{ cm}^{-1}$ and $\sim 3450\text{ cm}^{-1}$ (angular deformation of O-H and N-H) which is consistent with the occurrence of hydrogen bonding between BSA and functional groups in the spatial proximity of surfactants. In addition, in the NLC-BSA spectra, the specific values of the amide I band, were slightly shifted compared to pure BSA. These shifts can be attributed to changes in the protein structure (e.g., changes in the secondary structure - increase in the number of regions with α -helix conformation), as well as to the occurrence of weak hydrogen bonds formed between BSA and the functional groups of surfactants used in the preparation of NLC. The changes in protein structure are consistent with the results in the literature [7].

Fluorescence spectroscopy

The NLC-II-BSA systems exhibited a significantly stronger emission profile than that of native/pure BSA, dependent on the concentration of protein used for the NLC coating (Figure 4). These enhancements can be attributed on the one hand to the nanometric effect, and on the other hand due to the amount of BSA used for the NLC coating.

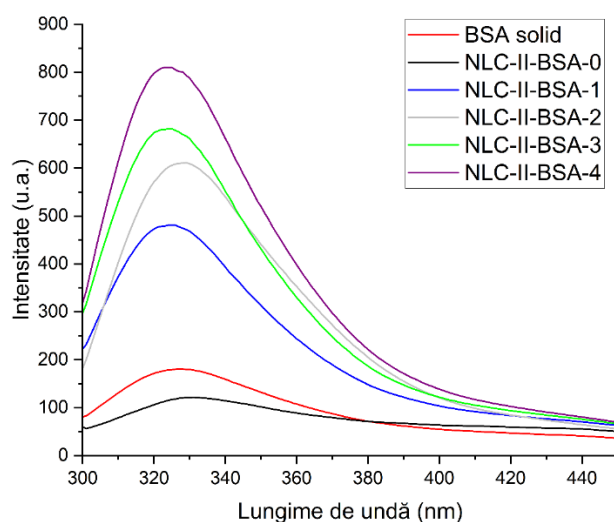


Figure 4: Fluorescent emission spectra of NLC-II-BSA-1/2/3/4 compared with NLC without BSA (NLC-II-BSA-0) and BSA.

8.2. Lipid nanocarriers coated with bovine serum albumin and loaded with piperine

Dimensions and morphological aspects

All prepared NLCs hybrids exhibited an average size < 140 nm, considered suitable for nanocarriers intended for drug delivery. In addition, the physical stability was maintained at a high level for all BSA-coated NLC-Pip, with Zeta potential values recorded around -60 mV. The spherical morphology of BSA-coated NLC-Pip-BSA and non-BSA-coated NLC-Pip was observed in STEM micrographs (Figure 5).

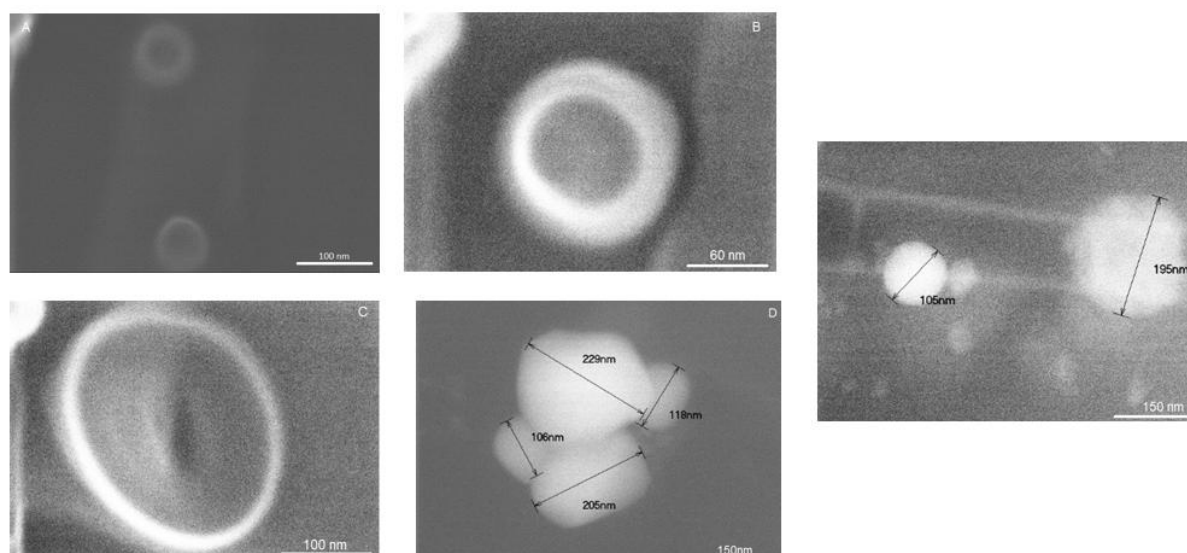


Figure 5: STEM images of NLC-III-Pip-BSA-3 showing BSA corona formation on the surface of NLC particles (A-C); STEM images of NLC-III-BSA-0 showing spherical morphology and diameter according to DLS analysis (D,E)

Spectral characterization

The FTIR spectra are similar to those of samples that were not loaded with piperine. On the other hand, major differences can be observed in the fluorescence spectra (Figure 6). First, there is the disappearance of the emission maximum at 325 nm, corresponding to BSA, a phenomenon called fluorescence quenching which refers to any process that reduces the fluorescence intensity of a sample, such as excited-state reactions, energy transfers, ground-state complex formation or collision phenomena [8]. Simultaneously it is observed that a BSA concentration-dependent fluorescent emission maximum occurs at about 430 nm, which is in fact the fluorescent emission of piperine. These changes suggest an energy transfer from BSA to Pip via dipol-dipol intermolecular interactions.

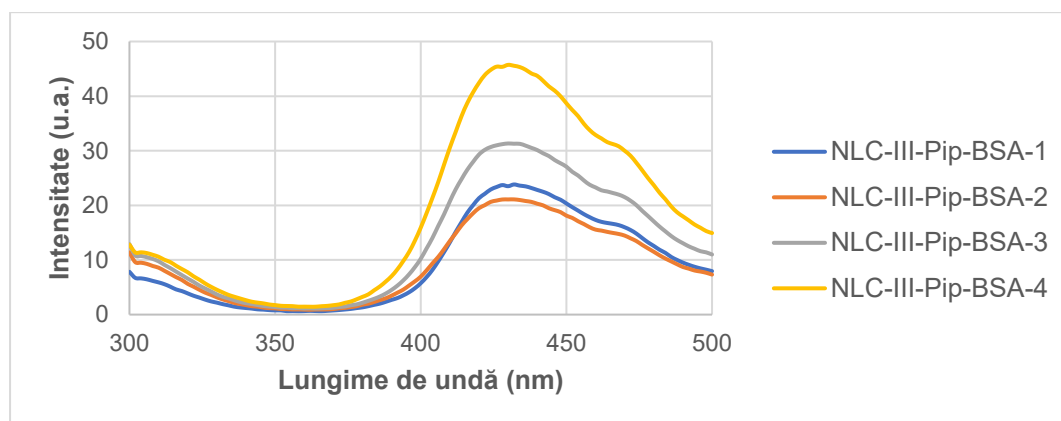


Figure 6: Fluorescence emission spectra of NLC-Pip-BSA

8.3. *In vitro* testing of conventional and BSA-coated NLCs

In vitro determination of antioxidant activity

The antioxidant activity of the NLC-III-Pip carriers was evaluated using the DPPH method at different NLC:DPPH dispersion ratios. The experimental results clearly show a dependence of the DPPH radical inhibition capacity on the NLC:DPPH dispersion ratio, such that a 4:1 volumetric ratio leads to an annihilation of radical species up to ~56%.

In vitro release studies of Piperine from NLC systems with and without BSA coating

The *in vitro* release profiles of piperine (Figure 7) show a rapid release of piperine, complete within 5 hours, which can be attributed to the large specific surface area and negative surface charge. Using several kinetic models, the obtained data were evaluated using several models. Thus, the kinetics of the release of Pip from NLC-III-Pip best fits the Higuchi model, while in the case of NLC-III-Pip-BSA the closest model is Peppas-Korsmeyer, and the mechanism of Pip release from NLC is governed by a Fickian-type diffusion.

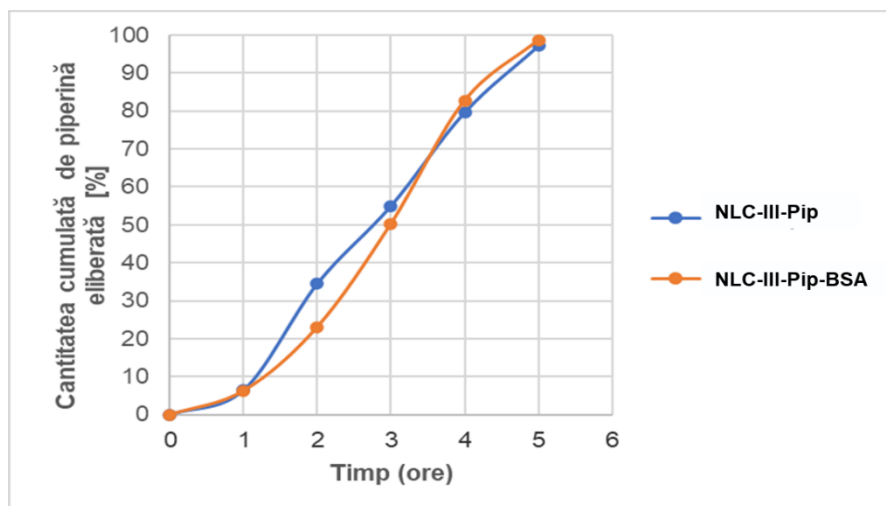


Figure 7: Comparative release profile of Piperine from NLC with/without BSA coating

8.4. Antitumor properties of NLC-Pip compared to BSA-decorated NLC-Pip

The NLC-III-Pip and NLC-III-Pip-BSA-3 formulations were evaluated in terms of biological functionality, by cytotoxicity (MTS and RTCA assays), apoptosis on tumor cells and cell cycle on normal versus breast, ovarian and colon cancer cells (flow cytometry analysis).

In vitro cytotoxicity determined for ovarian, breast and colon tumor cell lines

Given the presence of several phytochemical compounds in the lipid nanocarriers developed in this study, in addition to the tumor cells tested - colon, breast and ovarian, which were incubated for 24 hours, the influence of NLC on the viability of normal human umbilical vein endothelial cells (HUVEC) was also investigated. The anti-tumor efficacy of NLC-Pip/NLC-Pip-BSA was evaluated in comparison with two types of drugs with known chemotherapeutic activity used to treat several types of cancer - DOX and Cisplatin (Cis-Pt). All formulations showed a concentration-dependent effect, with cytotoxicity increasing proportionally with NLC-Pip/NLC-Pip-BSA concentration.

In LoVo cells, treatment with concentrations of 400 $\mu\text{g/mL}$ shows that nanostructured lipid transporters induce advanced cell death (e.g. $15.73\% \pm 0.82$ cell viability for NLC-Pip and $21.95\% \pm 1.06$ for NLC-Pip-BSA), comparable and even more pronounced in the case of NLC-Pip, compared to the cytotoxicity induced by treatment with the chemotherapeutic drug Cis-Pt (Figure 8). The results show a pronounced cytotoxic response for NLC-Pip treatment of 400 $\mu\text{g/mL}$ of the MCF-7 breast cancer cell lines, i.e., cell viability of $17.18\% \pm 0.35$ for NLC-Pip compared to $18.01\% \pm 0.93$ for the chemotherapeutic drug doxorubicin. Compared with the other two tumor lines, treatment with NLC resulted in a somewhat higher survival rate, e.g., $23.71\% \pm 1.59$ cell viability for NLC-Pip and $41.81\% \pm 1.33$ for NLC-Pip-BSA. However, the

cytotoxic efficacy induced by NLC was higher than the toxicity induced by the chemotherapeutic drug, Cisplatin (cell viability of $32.82\% \pm 1.40$).

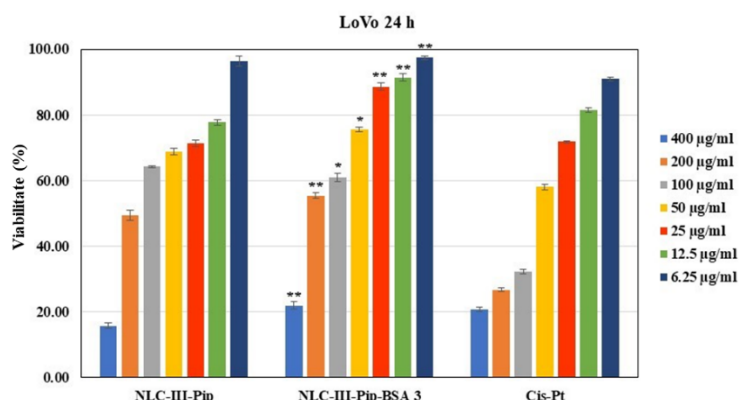


Figure 8: LoVo cell viability

The results of the MTS analysis were complemented by RTCA analysis which involves quantitative readout of cell counts and monitoring of proliferation by a real-time control. In the case of LoVo cells, this method confirms the advanced cytotoxicity induced by NLC-Pip and NLC-Pip-BSA, slightly more pronounced for NLC-Pip than for BSA-coated NLC-Pip, as 100 and 200 µg/mL NLC concentrations drastically reduced cell survival, whereas for the other two cell lines cell death is observed only for 200 µg/mL concentrations.

In addition, the IC_{50} values determined for each formulation show that piperine-loaded NLCs have cytotoxic activity against all cancer cell lines, with values close to those of cytostatic drugs.

Influence of NLC-Pip and NLC-Pip-BSA on tumor cell apoptosis

Evaluation of the apoptotic process in tumor cells shows that treating LoVo tumor cells for 24 hours with NLC-Pip (10 µg/mL) and NLC-Pip-BSA (100 µg/mL) increased apoptosis by 1.5-fold and 2-fold, respectively, whereas in MCF-7 tumor cells this process was enhanced approximately 8-fold for NLC-III-Pip-treated cells and 11-fold for NLC-III-Pip-BSA-3 cells, respectively (Figure 9). Treatment of SKOV-3 ovarian tumor cells for 24 h with NLC-III-Pip at a concentration of 10 µg/mL induced a 2-fold increase in apoptosis compared to the control and acts similarly to NLC-III-Pip-BSA-3 at a concentration of 100 µg/mL.

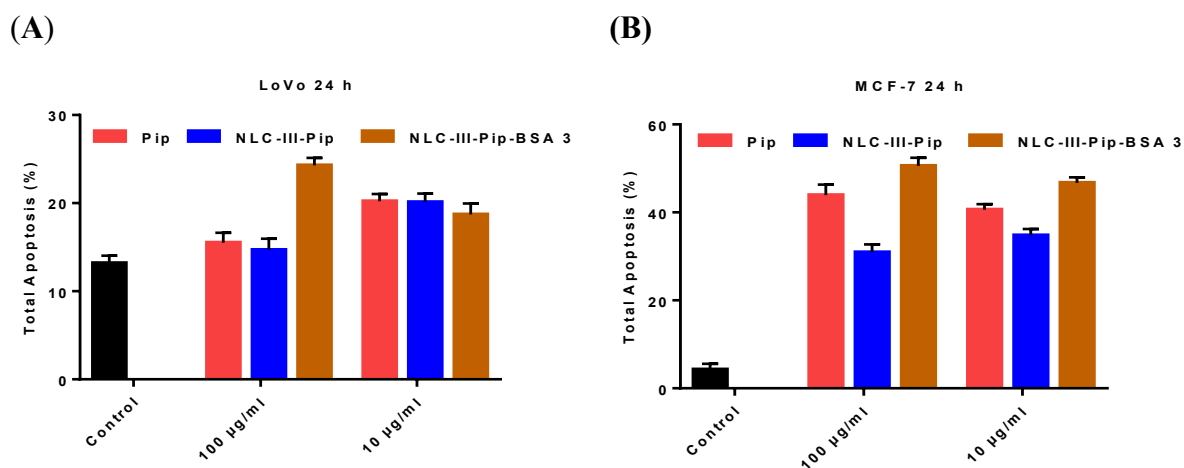


Figure 9: Apoptosis in LoVo cells (A); MCF-7 cells (B);

Influence of piperine-loaded hybrid NLCs on the cell cycle of normal and tumor cells

The effect induced by the hybrid nanostructured lipid transporters on the cell cycle of different tumor cells was comparatively analyzed by flow cytometry. In LoVo cells, concentrations of 100 µg/mL NLC-III-Pip and NLC-III-Pip-BSA-3, respectively, after 48 h treatment, provided a similar distribution of cell cycle phases. For NLC-III-Pip-BSA-3 a significant decrease in the proliferative S phase was reported, e.g. S = 43.6%, compared to the control, for which the S value was 75.07%.

Application of NLC-III-Pip-BSA-3 to MCF-7 tumor cells resulted in a decrease in proliferative S-phase (e.g., 23.76% for a concentration of 10 µg/mL and 21.8% for a concentration of 100 µg/mL) compared to control (S = 39.45%). Although treatment with NLC-III-Pip after 24 h did not significantly influence the cell cycle of MCF-7 cells, after 48 h of treatment, NLC-III-Pip (100 µg/mL) becomes more effective in reducing the proliferative S phase.

Treatment of SKOV-3 ovarian tumor cells with conventional and hybrid NLC-III-Pip showed a remarkable tumor suppressive effect, evidenced by a significant decrease in S-phase. NLC-III-Pip (100 µg/mL) and NLC-III-Pip-BSA-3 (100 µg/mL) reduced the S-phase of the cell cycle after 24 h of treatment, but after 48 h, the maximum S-phase inhibitory effect (S = 1.13%) was exerted by NLC-III-Pip (100 µg/mL) compared to the control (S = 22.4%).

8.5. Conclusions

This chapter reports the obtaining and testing of a novel BSA-coated NLC-type DDS for enhanced cellular internalization of piperine into various tumor cells. The BSA coating was achieved by creating interactions of non-covalent nature between the ionic surfactant shell and

the protein. Spectral analysis showed that simultaneously with BSA binding the protein undergoes a modification of its native structure. In addition, in piperine-containing systems, a relocation of the fluorescence source also occurs, with quenching of albumin fluorescence, and the appearance of the piperine emission maximum.

Cytotoxicity assays showed that synthesized NLCs induced advanced cell death in LoVo and MCF-7 cells, comparable even to cytostatic drugs, while flow cytometry analyses show that cell death is induced by different mechanisms.

CHAPTER IX

Hybrid Albumin-Decorated Lipid-Nanocarrier-Mediated Delivery of Polyphenol-Rich *Sambucus nigra* L.

Chapter IX presents the synthesis of hybrid NLCs encapsulating black elderberry (*Sambucus nigra*) extract, an extract in phytochemicals, especially polyphenols and anocyanins, but which have very low bioavailability, which implicitly leads to a diminished therapeutic potential. This chapter has a high degree of originality, as this study - **unexplored in the literature** - presents the combinatorial potential of *Sambucus nigra* and albumin-decorated NLCs as bioactive phytochemical nanocarrier that can support targeted anti-tumor therapy, with therapeutic efficacy evaluated in parallel with the conventional chemotherapeutics, Doxorubicin and Cisplatin.

9.1. Physico-chemical characterization of NLCs loaded with *Sambucus nigra* extract

For the systems encapsulating *Sambucus nigra*, lipid cores were used, one consisting of natural lipids such as MSG, coconut butter (CB) and sage oil (NLC-I series), and the second one consisting of a synthetic ester (mentil laurate), associated with coconut butter and glycerol monostearate (NLC-II series), stabilized by a surfactant mixture of sodium cholate, phosphatidylcholine and Tween 20 (Table 6).

Tabel 6: Proposed formulations for the encapsulation of *Sambucus nigra* extract

Sample name	Lipid phase, g				Aqueous phase*, g			EE, %
	MSG	CB	US	LM	NaCh	PC	TW20	
NLC-I- <i>SambucusN</i>	3,5	3,5	3	-	0,3	0,7	1,5	88,67 ± 4,746
NLC-II- <i>SambucusN</i>	3,5	3,5	1,5	1,5	0,3	0,7	1,5	74,49 ± 6,701

* due to its hydrophilic character, *Sambucus nigra* extract (1 g) was added in the aqueous phase

DLS characterization revealed free NLC systems with diameters of about 125 nm, which increase slightly during the incorporation process of the phytochemical extract. PdI values some lipid populations with a relatively homogeneous and monodispersed distribution. In terms of Zeta potential, all NLCs present strongly negative values. In traditional systems the Zeta

potential values are more electronegative than -50 mV, while after BSA coating, these values show a tendency to decrease in absolute value (between -30 and -40 mV), due to neutralization of surface charges.

9.2. FTIR and fluorescence spectroscopy analysis of NLC-*SambucusN*-BSA

FTIR analysis leads to spectra of similar general shape with vibration bands characteristic of the system components. In the case of hybrid formulations, the presence of the two bands of BSA is observed at values different from the characteristic values of pure BSA, indicating a modification of the secondary structure. This observation is also consistent with the enhancement of the O-H and N-H vibration bands, indicating the occurrence of hydrogen bonding.

In regards to fluorescence spectroscopy, free hybrid systems show an enhancement of fluorescence emission compared to BSA, which is characteristic of nanosized carriers that allow more interaction centers and therefore generate a more intense fluorescence effect [9]. By loading with *SambucusN* extract a fluorescence quenching occurs, which decreases the fluorescent emission of NLC by up to two times. According to the literature, this decrease occurs due to the formation of hydrogen bonds between the hydroxyl groups of the polyphenols and the amino acid residues of BSA [10].

9.3. *In vitro* evaluation of antioxidant activity

In vitro antioxidant activity of the synthesized carriers was evaluated using the ABTS method. The antioxidant activity of NLC-I and -II-*SambucusN* was significantly enhanced by albumin coating. Thus, the maximum ABTS^{•+} cation radical annihilation potency determined for the two categories of NLC-hybrids was $89.81 \pm 4.84\%$ and $86.01 \pm 3.07\%$ for NLC-I and -II-*SambucusN* coated with the biopolymer BSA, compared with $74.47 \pm 1.15\%$ and $81.93 \pm 2.70\%$ determined for NLC-I and -II-*SambucusN* without BSA (Figure 10).

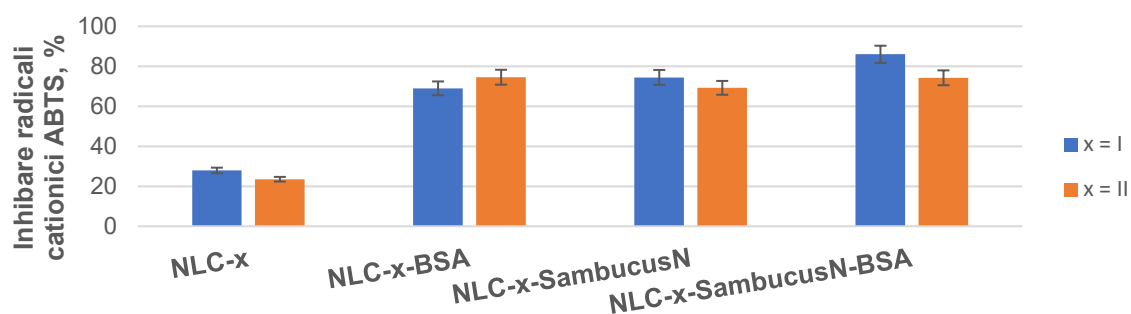


Figure 10: ABTS●+ radical cation scavenging activity by NLC-I- and -II- SambucusN with and without BSA

The IC_{50} values for the two representative NLCs were 1.483 mg/mL (NLC-I-*SambucusN*-BSA) and 0.973 mg/mL (NLC-II-*SambucusN*-BSA). These results reveal the superior antioxidant activity of NLC-II-*SambucusN*-BSA, which includes menthyl laurate in its composition probably due to the better uptake of some lipophilic flavonoids from *SambucusN* in lipid mixtures with menthol ester.

9.4. *In vitro* testing of the anti-tumor efficacy of obtained NLC systems

The synthesized formulations were evaluated for their biological functionality in a series of assays, including cytotoxicity assays (MTS and RTCA), induction of apoptosis in tumor cells and comparative cell cycle analysis between normal cells and breast, ovarian and colon cancer cells using flow cytometry.

9.4.1. Cytotoxicity of conventional and hybrid BSA-decorated NLC-*SambucusN* cytotoxicity

Tests on normal HUVEC cells showed that most of the formulations obtained are biocompatible. On the other hand. In LoVo cells (Figure 11), an advanced cytotoxicity was observed upon treatment with 100 μ g/mL NLC-I-*SambucusN*-BSA for 48 h treatment period ($21.81 \pm 1.18\%$). In MCF-7 cells, NLC-I induces advanced cell death, so that after 48 hour of treatment with 400 μ g/mL, cell viability is $10.32 \pm 0.97\%$. In SKOV-3 cells, the efficiency of NLC against proliferation is quite low.

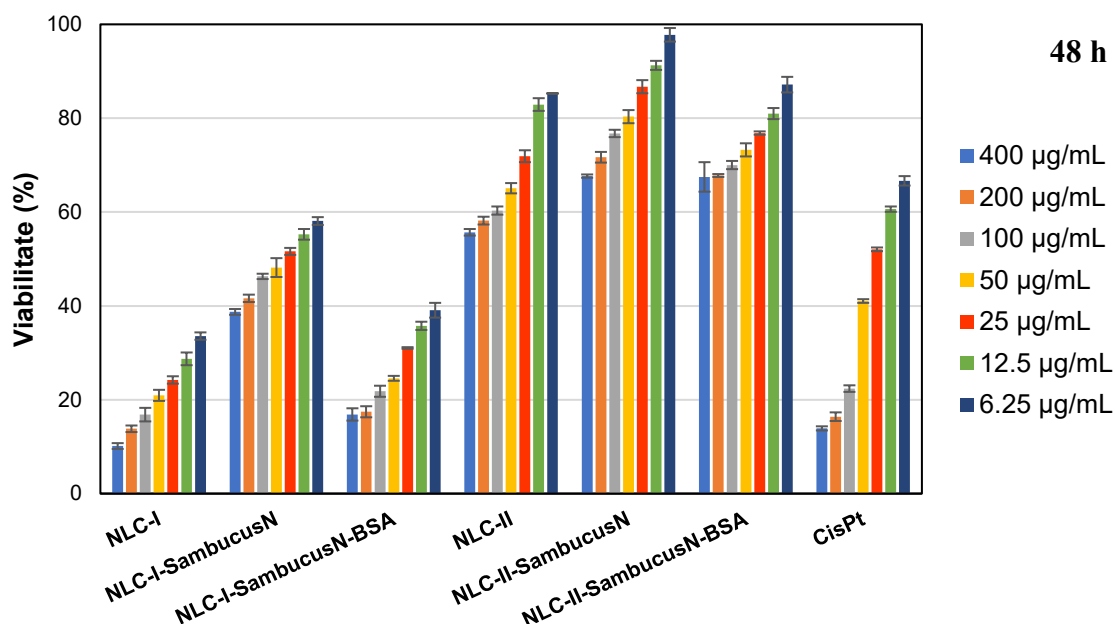


Figura 11: Efectul NLC conven ionale  i hibride asupra celulelor tumorale LoVo, dup  48 de ore

9.4.2. Real-time analysis of tumor cells treated with NLC-*SambucusN* systems

Proliferation curves recorded over an extended period, from 0 to 243 h, were obtained after treatment of LoVo, MCF-7 and SKOV-3 tumor cells with concentrations of NLCs ranging from 12.5 to 200 µg/mL.

The most pronounced antitumor action was on the LoVo cell line. Among the NLCs tested, NLC-I-*SambucusN*-BSA showed a markedly superior ability to halt the proliferation of LoVo tumor cells.

Regarding MCF-7 tumor cells, at a concentration of 200 µg/mL, all formulations produce advanced cytotoxicity on tumor cells, whereas at 100 µg/mL, NLC-I-*SambucusN* with and without BSA is more effective in inhibiting MCF-7 tumor cell proliferation if the treatment duration exceeds 48 h.

A relatively similar trend was observed for SKOV-3 cells, where NLC-I-*SambucusN* was the most effective at all concentrations tested. As for NLC-II, containing mentil laurate, NLC-II-*SambucusN* and NLC-II-*SambucusN*-BSA significantly inhibited the proliferation of SKOV-3 tumor cells at a concentration of 100 µg/mL and 50 µg/mL respectively and prolonged treatment for more than 48 h.

9.4.3. Effect of albumin-decorated NLC-SambucusN on the apoptotic process

In order to analyze the toxic action of these compounds on normal cells, NLC was applied under the same conditions on normal HUVEC cells. The data show that NLC-I-*SambucusN*-BSA (24 h) and NLC-II-*SambucusN*-BSA (48 h) protect normal cells from entering apoptosis compared to the effect induced by NLC-I and NLC-II, irrespective of their time of action.

The results obtained with NLC-I and II-*SambucusN* treatments with and without BSA on LoVo tumor cells after 24 h of treatment, highlighted moderate values of about 18% apoptosis. In contrast, treatment of LoVo tumor cells for 24 or 48 h with the three NLC-II categories led to a 2 ÷ 4-fold increase in apoptotic process compared to untreated (control) cells.

Irrespective of the concentration used, all NLC-IIs prove to be more effective in apoptosis of MCF-7 tumor cells than the effect induced by the NLC-I series, especially for 24 h treatments. A prolonged 48 h treatment with NLC-I and NLC-I-*SambucusN* had a notable efficacy in apoptosis of MCF-7 cells; for example, the apoptotic process is enhanced 5-fold when using 50 µg/mL NLC compared to the control group..

Rezultatele determinate pentru celulele tumorale SKOV-3 (Figura 9.16D) au arătat că tratamente cu 50 µg/mL NLC-I, NLC-I-*SambucusN* și NLC-I-*SambucusN*-BSA activează procesul de apoptoză a celulelor tumorale ovariene atât după 24 h, cât și după 48 h. NLC-II acționează într-un mod similar, amplificând procesul apoptotic al celulelor tumorale comparativ cu controlul.

9.4.4. Influence of NLC-SambucusN and NLC-SambucusN-BSA on cell cycles

Results obtained by flow cytometry indicate that treatment with hybrid lipid nanocarriers with and without *SambucusN* extract does not significantly influence cell cycle phases in normal HUVECs. On the other hand, untreated LoVo tumor cells show a higher S phase, indicating an intense proliferation activity. When NLC-I, NLC-I-*SambucusN* and NLC-I-*SambucusN*-BSA are applied at concentrations of 50 µg/mL, they induce cell cycle arrest in the G1 phase of LoVo tumor cells.

Similarly, treatment of MCF-7 tumor cells with 50 µg/mL of NLC-I and NLC-II effectively arrests the cell cycle in G1 phase and induces a dramatic decrease in S phase. NLC-II-*SambucusN* and NLC-II-*SambucusN*-BSA demonstrate higher efficacy than the NLC type I series prepared with sage oil for both 24 h and 48 h.

All types of lipids and protein lipid nanocarriers act by reducing the S phase of SKOV-3 cells, accompanied by an increase in G2 phase. These results underline that NLC-I and NLC-

II could inhibit the proliferation of SKOV-3 tumor cells by blocking the cell cycle in G2 phase. Treatment of SKOV-3 cells for 48 hours with the three forms of NLC-I and NLC-II does not significantly alter the phases of the cell cycle distribution.

9.5. Conclusions

In this chapter, the synergistic effect of *Sambucus nigra* polyphenolic extract and BSA-coated hybrid nanostructured nanostructured BSA-coated lipid transporters as a targeted treatment system for colon, breast and ovarian cancer was analyzed for the first time. The formulations, based on two types of lipid cores, exhibited homogeneous nanometric dimensions and high colloidal stability. The NLC-I series systems incorporated the plant extract more efficiently and showed improved antioxidant activity enhanced by the presence of albumin. In vitro tests showed a pronounced cytotoxic effect on tumor cells (LoVo, SKOV-3, MCF-7), comparable to conventional treatments, by inducing apoptosis and blocking the cell cycle in G1 or G2 phases, depending on cell type and formulation.

CHAPTER X

Final conclusions and personal contributions

10.1. Final conclusions

The original research, materialized in the results presented in chapters VI ÷ IX, revealed the following:

In **Chapter VI** “*Extraction of piperine and synthesis of mentil laurate*”, important raw materials for the development of hybrid nanosystems with remarkable abilities for targeted anti-tumor therapy were obtained. Thus, the bioactive alkaloid - Piperine was isolated from black pepper berries by a solid-liquid extraction method and recrystallized from isopropanol, and the menthyl laurate was obtained by a Steglich esterification. Both compounds were characterized by classical organic chemistry methods and their structures were confirmed by spectroscopic techniques (FTIR and NMR).

Chapter VII “*Preliminary NLC Composition Optimization Studies*” evaluated the behavior of varying compositions of lipids and surfactants (ionic, nonionic and amphiphilic), necessary to balance interactions of a physical nature (e.g. hydrophobic forces, electrostatic attractions, hydrogen bonding) and to establish effective interactions with the BSA biopolymer. DLS analysis results (determined both after synthesis and after two weeks of storage) showed that NLC formulations obtained with higher concentration of ionic surfactants (NaCh and PC) tend to result in lipid nanocarrier systems with smaller diameters, and a volumetric ratio between NLC dispersion and BSA solution of 1:1 is required for a total coverage of nanocarriers.

Chapter VIII “*Nanostructured bovine serum albumin-coated nanostructured lipid transporters capable of altering the cell cycle in different cancer types*” included original results on the development and characterization of conventional NLCs and hybrid NLCs encapsulating piperine for enhanced cellular internalization into different tumor cells. The synthesized systems had dimensions ranged in size from 50 to 400 nm, spherical morphology and sufficiently negative Zeta potential to ensure adequate stability. Encapsulation efficiency was high (~81%), and spectral analysis confirmed hydrophobic and electrostatic interactions between NLC and albumin, and also revealed structural changes in BSA occurring during these interactions. The obtained formulations exhibited cytotoxicity and apoptosis-stimulating effects, particularly in LoVo and MCF-7 cells, with results comparable to those of cytostatic drugs. In addition, a significant inhibition of the S-phase of the cell cycle was observed,

highlighting a possible active tumor targeting effect. All these results support the potential of these nanosystems as efficient vectors for in vivo delivery of piperine.

Chapter IX “*Lipid nanocarriers decorated with bovine serum albumin for the delivery of Sambucus nigra extract*” presents the production and characterization of conventional and hybrid NLC systems in which *Sambucus nigra* extract was encapsulated. These systems exhibited <160 nm dimensions, homogeneous distribution and high encapsulation efficiency of the extract, especially in the presence of albumin. Functionalization with albumin resulted in enhanced antioxidant activity and favorably influenced the biological response in tumor cell line assays. The obtained nanocarriers induced apoptosis and cell cycle arrest in colon, breast and ovarian cells, in some cases with effects comparable to Cisplatin. These results suggest promising potential for the use of these systems in synergistic and targeted oncologic therapies.

10.2. Original contributions

Original contributions of the research developed in this PhD thesis:

I. Obtaining novel lipid-protein delivery systems with improved delivery and targeted release abilities of phytochemical active principles. The present PhD thesis makes notable contributions on the exploitation of bioactive phytochemical mixtures, co-opted in hybrid (lipid-protein) NLC systems, in future therapeutic strategies to improve bioavailability and thus therapeutic effects. The obtained results encourage the combinatorial potential of albumin-decorated NLCs loaded with phytochemicals (Piperine, *Sambucus nigra*) as an effective platform supporting the destruction process of different tumor cells, either by activating cell cycle blocking mechanisms at the different steps controlling the cell cycle progression or by activating apoptotic pathways.

II. Demonstration of anti-tumor efficacy by in vitro assays of cell viability, cell cycle damage and apoptosis. The comparative anti-tumor effect of the developed hybrid NLCs was performed on different tumor cell lines (breast cancer/MCF-7, colon cancer/LoVo and ovarian adenocarcinoma/SKOV-3 cells). Their efficacy was evaluated against the action of two cytostatic drugs, Cisplatin and Doxorubicin. The application of the developed NLCs to tumor cell lines, revealed a different internalization depending on the colon, mammary and ovarian tumor cell line, with the potential use of distinct apoptotic pathways.

Publications

Articles

1. Sabina Ion, Florentina Olănescu, Florina Teodorescu, **Robert Țincu**, Daniela Gheorghe, Vasile I. Pârvulescu, Mădălina Tudorache, „DES-Based Biocatalysis as a Green Alternative for the l-menthyl Ester Production Based on l-menthol Acylation”, *Molecules*, **2022**, 27(6) 5273, doi: 10.3390/molecules27165273 (IF = 4,6)
2. **Robert Țincu**, Mirela Mihăilă, Mirela Bostan, Florina Teodorescu, Daniela Istrati, Nicoleta Badea, Ioana Lăcătușu, „Novel Bovine Serum Albumin-Decorated–Nanostructured Lipid Carriers Able to Modulate Apoptosis and Cell-Cycle Response in Ovarian, Breast, and Colon Tumoral Cells”, *Pharmaceutics*, **2023**, 15(4), 1125, doi: 10.3390/pharmaceutics15041125 (IF = 4,9)
3. **Robert Țincu**, Mirela Mihăilă, Marinela Bostan, Daniela Istrati, Nicoleta Badea, Ioana Lăcătușu, „Hybrid Albumin-Decorated Lipid-Nanocarrier-Mediated Delivery of Polyphenol-Rich *Sambucus nigra* L. in a Potential Multiple Antitumoural Therapy”, *International Journal of Molecular Sciences*, **2024**, 25(20), 11206, doi: 10.3390/ijms252011206 (IF = 4,9)
4. **Robert Țincu**, Ioana Sumedrea, Mădălina Tudorache, Florina Teodorescu, „Enzymatic hydrolysis of fatty acids menthyl esters in the presence of lipase enzyme”, *U.P.B. Scientific Bulletin, Series B*, **2025**, 48, 23-34 (IF = 0,6)

Conferences

1. **Robert Țincu**, Florina Teodorescu, Nicoleta Badea, Daniela Istrati, Ioana Lăcătușu, „Novel Hybrid Nanostructured Lipid Carrier for Piperine Encapsulation”, *22nd Romanian Internațional Conference on Chemistry and Chemical Engineering (RICCCE 22)*, **7-9.09.2022**, Sinaia, România;
2. **Robert Țincu**, Florina Teodorescu, „Fatty acid menthol esters – synthesis and characterization”, *Conferința Națională de Chimie – ediția XXXVI*, 04-07.10.2022, Călimănești, România.

References

1. Sultana, A.; Zare, M.; Thomas, V.; Kumar, T.S.S.; Ramakrishna, S. Nano-Based Drug Delivery Systems: Conventional Drug Delivery Routes, Recent Developments and Future Prospects. *Med Drug Discov* **2022**, *15*, 100134, doi:10.1016/j.medidd.2022.100134.
2. Chen, Q.; Yang, Z.; Liu, H.; Man, J.; Oladejo, A.O.; Ibrahim, S.; Wang, S.; Hao, B. Novel Drug Delivery Systems: An Important Direction for Drug Innovation Research and Development. *Pharmaceutics* **2024**, *16*, 674, doi:10.3390/pharmaceutics16050674.
3. Zi, Y.; Yang, K.; He, J.; Wu, Z.; Liu, J.; Zhang, W. Strategies to Enhance Drug Delivery to Solid Tumors by Harnessing the EPR Effects and Alternative Targeting Mechanisms. *Adv Drug Deliv Rev* **2022**, *188*, 114449, doi:10.1016/j.addr.2022.114449.
4. Nichols, J.W.; Bae, Y.H. EPR: Evidence and Fallacy. *Journal of Controlled Release* **2014**, *190*, 451–464, doi:10.1016/j.jconrel.2014.03.057.
5. Dutta, B.; Barick, K.C.; Hassan, P.A. Recent Advances in Active Targeting of Nanomaterials for Anticancer Drug Delivery. *Adv Colloid Interface Sci* **2021**, *296*, 102509, doi:10.1016/j.cis.2021.102509.
6. Khaledian, S.; Dayani, M.; Fatahian, A.; Fatahian, R.; Martinez, F. Efficiency of Lipid-Based Nano Drug Delivery Systems in Crossing the Blood–Brain Barrier: A Review. *J Mol Liq* **2022**, *346*, 118278, doi:10.1016/j.molliq.2021.118278.
7. Müller, R.H.; Radtke, M.; Wissing, S.A. Nanostructured Lipid Matrices for Improved Microencapsulation of Drugs. *Int J Pharm* **2002**, *242*, 121–128, doi:10.1016/S0378-5173(02)00180-1.
8. Agrawal, Y.; Petkar, K.C.; Sawant, K.K. Development, Evaluation and Clinical Studies of Acitretin Loaded Nanostructured Lipid Carriers for Topical Treatment of Psoriasis. *Int J Pharm* **2010**, *401*, 93–102, doi:10.1016/j.ijpharm.2010.09.007.
9. Van de Sande, L.; Cosyns, S.; Willaert, W.; Ceelen, W. Albumin-Based Cancer Therapeutics for Intraperitoneal Drug Delivery: A Review. *Drug Deliv* **2020**, *27*, 40–53, doi:10.1080/10717544.2019.1704945.
10. Asrorov, A.M.; Mukhamedov, N.; Kayumov, M.; Sh. Yashinov, A.; Wali, A.; Yili, A.; Mirzaakhmedov, S.Ya.; Huang, Y. Albumin Is a Reliable Drug-Delivering Molecule:

Highlighting Points in Cancer Therapy. *Med Drug Discov* **2024**, *22*, 100186, doi:10.1016/j.medidd.2024.100186.

11. Neises, B.; Steglich, W. Simple Method for the Esterification of Carboxylic Acids. *Angewandte Chemie International Edition in English* **1978**, *17*, 522–524, doi:10.1002/anie.197805221.

12. Milenković, A.; Stanojević, L. Black Pepper: Chemical Composition and Biological Activities. *Advanced Technologies* **2021**, *10*, 40–50, doi:10.5937/savteh2102040M.

13. Elmowafy, M.; Al-Sanea, M.M. Nanostructured Lipid Carriers (NLCs) as Drug Delivery Platform: Advances in Formulation and Delivery Strategies. *Saudi Pharmaceutical Journal* **2021**, *29*, 999–1012, doi:10.1016/j.jsps.2021.07.015.

14. Javed, S.; Mangla, B.; Almoshari, Y.; Sultan, M.H.; Ahsan, W. Nanostructured Lipid Carrier System: A Compendium of Their Formulation Development Approaches, Optimization Strategies by Quality by Design, and Recent Applications in Drug Delivery. *Nanotechnol Rev* **2022**, *11*, 1744–1777, doi:10.1515/NTREV-2022-0109/ASSET/GRAPHIC/J_NTREV-2022-0109_FIG_004.JPG.

15. H. Muller, R.; Mader, K.; Gohla, S. Solid Lipid Nanoparticles (SLN) for Controlled Drug Delivery ± a Review of the State of the Art. **2000**, *50*, 161–177.

16. Kim, M.H.; Kim, K.T.; Sohn, S.Y.; Lee, J.Y.; Lee, C.H.; Yang, H.; Lee, B.K.; Lee, K.W.; Kim, D.D. Formulation And Evaluation Of Nanostructured Lipid Carriers (NLCs) Of 20(S)-Protopanaxadiol (PPD) By Box-Behnken Design. *Int J Nanomedicine* **2019**, *14*, 8509, doi:10.2147/IJN.S215835.

17. Wang, W.; Huang, Z.; Li, Y.; Wang, W.; Shi, J.; Fu, F.; Huang, Y.; Pan, X.; Wu, C. Impact of Particle Size and PH on Protein Corona Formation of Solid Lipid Nanoparticles: A Proof-of-Concept Study. *Acta Pharm Sin B* **2021**, *11*, 1030–1046, doi:10.1016/j.apsb.2020.10.023.

18. Zhang, J.; Chen, L.; Zeng, B.; Kang, Q.; Dai, L. Study on the Binding of Chloroamphenicol with Bovine Serum Albumin by Fluorescence and UV-Vis Spectroscopy. *Spectrochim Acta A Mol Biomol Spectrosc* **2013**, *105*, 74–79, doi:10.1016/j.saa.2012.11.064.

19. Nishihira, V.S.K.; Rubim, A.M.; Brondani, M.; dos Santos, J.T.; Pohl, A.R.; Friedrich, J.F.; de Lara, J.D.; Nunes, C.M.; Feksa, L.R.; Simão, E.; et al. In Vitro and in Silico Protein

Corona Formation Evaluation of Curcumin and Capsaicin Loaded-Solid Lipid Nanoparticles. *Toxicology in Vitro* **2019**, *61*, 104598, doi:10.1016/J.TIV.2019.104598.

20. Yu, X.; Cai, X.; Luo, L.; Wang, J.; Ma, M.; Wang, M.; Zeng, L. Influence of Tea Polyphenol and Bovine Serum Albumin on Tea Cream Formation by Multiple Spectroscopy Methods and Molecular Docking. *Food Chem* **2020**, *333*, 127432, doi:10.1016/J.FOODCHEM.2020.127432.